

Energy Efficiency in the Low-SNR Regime under ¹ Queueing Constraints and Channel Uncertainty

Deli Qiao, Mustafa Cenk Gursoy, and Senem Velipasalar

Abstract

Energy efficiency of fixed-rate transmissions is studied in the presence of queueing constraints and channel uncertainty. Without assuming any knowledge on the channel side information (CSI) at transmitter or receiver, the channel coefficients are estimated at the receiver via minimum mean-square-error (MMSE) estimation with the aid of training symbols. We assume that the system operates under statistical queueing constraints in the form of limitations on buffer violation probabilities. The optimal fraction of power allocated to training is identified. Energy efficiency is investigated by obtaining the bit energy required at zero spectral efficiency and the wideband slope in both low-power and wideband regimes. In particular, it is shown that the bit energy increases without bound in the low-power regime, which is also equivalent to the wideband regime with rich multipath fading, as the average power vanishes. On the other hand, the minimum bit energy and wideband slope expressions are found in the wideband regime with multipath sparsity. Moreover, the bit energy–spectral efficiency tradeoff is studied for a special case in the wideband regime. Through the analysis, the impact upon the energy efficiency of multipath sparsity and richness is characterized, and comparisons with the case when perfect CSI is available at the receiver are provided.

Index Terms: bit energy, channel estimation, effective capacity, energy efficiency, fading channels, fixed-rate transmission, imperfect channel knowledge, low-power regime, minimum bit energy, QoS constraints, spectral efficiency, wideband regime, wideband slope.

The authors are with the Department of Electrical Engineering, University of Nebraska-Lincoln, Lincoln, NE, 68588 (e-mails: dqiao726@huskers.unl.edu, gursoy@engr.unl.edu, velipasa@engr.unl.edu).

This work was supported by the National Science Foundation under Grants CCF – 0546384 (CAREER) and CNS – 0834753.

I. INTRODUCTION

The two key characteristics of wireless communications that most greatly impact system design and performance are 1) the randomly-varying channel conditions and 2) limited energy resources. In wireless systems, the power of the received signal fluctuates randomly over time due to mobility, changing environment, and multipath fading caused by the constructive and destructive superimposition of the multipath signal components [26]. These random changes in the received signal strength lead to variations in the instantaneous data rates that can be supported by the channel. In addition, mobile wireless systems can only be equipped with limited energy resources, and hence energy efficient operation is a crucial requirement in most cases.

To measure and compare the energy efficiencies of different systems and transmission schemes, one can choose as a metric the energy required to reliably send one bit of information. Information-theoretic studies show that energy-per-bit requirement is generally minimized, and hence the energy efficiency is maximized, if the system operates at low signal-to-noise ratio (SNR) levels and hence in the low-power or wideband regimes. Recently, Verdú in [1] has determined the minimum bit energy required for reliable communication over a general class of channels, and studied of the spectral efficiency–bit energy tradeoff in the wideband regime while also providing novel tools that are useful for analysis at low SNRS.

In many wireless communication systems, in addition to energy-efficient operation, satisfying certain quality of service (QoS) requirements is of paramount importance in providing acceptable performance and quality. For instance, in voice over IP (VoIP), interactive-video (e.g., videoconferencing), and streaming-video applications in wireless systems, latency is a key QoS metric and should not exceed certain levels [27]. On the other hand, wireless channels, as described above, are characterized by random changes in the channel, and such volatile conditions present significant challenges in providing QoS guarantees. In most cases, statistical, rather than deterministic, QoS assurances can be given.

In summary, it is vital for an important class of wireless systems to operate efficiently while also satisfying QoS requirements (e.g., latency, buffer violation probability). Information theory provides the ultimate performance limits and identifies the most efficient use of resources. However, information-theoretic studies and Shannon capacity formulation generally do not address delay and quality of service (QoS) constraints [2]. Recently, Wu and Negi in [4] defined the effective capacity as the maximum constant arrival rate that a given time-varying service process can support while providing statistical QoS guarantees. Effective capacity formulation uses the large deviations theory and incorporates the statistical QoS constraints by capturing

the rate of decay of the buffer occupancy probability for large queue lengths. Hence, effective capacity can be regarded as the maximum throughput of a system operating under limitations on the buffer violation probability. In the absence of such limitations, effective capacity specializes to the ergodic capacity. At the other extreme in which deterministic, rather than statistical, limitations are imposed, effective capacity specializes to the delay-limited capacity [3]. Hence, in general, effective capacity formulation, by providing us the performance in the presence of soft constraints on the queue length, enables us to fill in the gap between the results obtained using ergodic and delay-limited capacities (see e.g., [14] for further discussion).

The analysis and application of effective capacity in various settings has attracted much interest recently (see e.g., [5]–[14] and references therein). For instance, Tang and Zhang in [7] considered the effective capacity when both the receiver and transmitter know the instantaneous channel gains, and derived the optimal power and rate adaptation technique that maximizes the system throughput under QoS constraints. These results are extended to multichannel communication systems in [8]. Liu *et al.* in [11] considered fixed-rate transmission schemes and analyzed the effective capacity and related resource requirements for Markov wireless channel models. In this work, the continuous-time Gilbert-Elliott channel with ON and OFF states is adopted as the channel model while assuming the fading coefficients as zero-mean Gaussian distributed. A study of cooperative networks operating under QoS constraints is provided in [12]. In [14], we have investigated the energy efficiency under QoS constraints by analyzing the normalized effective capacity (or equivalently the spectral efficiency) in the low-power and wideband regimes. We considered variable-rate/variable-power and variable-rate/fixed-power transmission schemes assuming the availability of channel side information at both the transmitter and receiver or only at the receiver.

In this paper, we study the energy efficiency in the presence of queueing constraints and channel uncertainty. We assume that the channel is not known by the transmitter and receiver prior to transmission, and is estimated imperfectly by the receiver through training. In our model, we incorporate statistical queueing constraints by employing the effective capacity formulation which provides the maximum throughput under limitations on buffer violation probabilities for large buffer sizes. Since the transmitter is assumed to not know the channel, fixed-rate transmission is considered.

The rest of the paper is organized as follows. Section II introduces the system model. In Section III, we briefly describe the notion of effective capacity and the spectral efficiency–bit energy tradeoff. Energy efficiency in the low-power regime is investigated in Section IV. In Section V, we analyze the energy efficiency in the wideband regime under the assumption of sparse multipath fading. Finally, Section VI

provides conclusions while proofs of several theorems are relegated to the Appendix.

II. SYSTEM MODEL

We consider a point-to-point wireless link in which there is one source and one destination. It is assumed that the source generates data sequences which are divided into frames of duration T . These data frames are initially stored in the buffer before they are transmitted over the wireless channel. The discrete-time channel input-output relation in the i^{th} symbol duration is given by

$$y[i] = h[i]x[i] + n[i] \quad i = 1, 2, \dots \quad (1)$$

where $x[i]$ and $y[i]$ denote the complex-valued channel input and output, respectively. We assume that the bandwidth available in the system is B and the channel input is subject to the following average energy constraint: $\mathbb{E}\{|x[i]|^2\} \leq \bar{P}/B$ for all i . Since the bandwidth is B , symbol rate is assumed to be B complex symbols per second, indicating that the average power of the system is constrained by \bar{P} . Above in (1), $n[i]$ is a zero-mean, circularly symmetric, complex Gaussian random variable with variance $\mathbb{E}\{|n[i]|^2\} = N_0$. The additive Gaussian noise samples $\{n[i]\}$ are assumed to form an independent and identically distributed (i.i.d.) sequence. Finally, $h[i]$, which denotes the channel fading coefficient, is assumed to be a zero-mean Gaussian random variable with variance $E\{|h|^2\} = \gamma$. We further assume that the fading coefficients stay constant during the frame duration of T seconds and have independent realizations for each frame. Hence, we basically consider a block-fading channel model. We also note that neither the transmitter nor the receiver has channel side information prior to transmission.

The system operates in two phases: training phase and data transmission phase. In the training phase, known pilot symbols are transmitted to enable the receiver to estimate the channel conditions, albeit imperfectly. We assume that minimum mean-square-error (MMSE) estimation is employed at the receiver to estimate the channel coefficient $h[i]$. Since the MMSE estimate depends only on the training energy and not on the training duration [20], it can be easily seen that transmission of a single pilot at every T seconds is optimal. Note that in every frame duration of T seconds, we have TB symbols and the overall available energy is $\bar{P}T$. We now assume that each frame consists of a pilot symbol and $TB - 1$ data symbols. The energies of the pilot and data symbols are

$$\mathcal{E}_t = \rho\bar{P}T, \quad \text{and} \quad \mathcal{E}_s = \frac{(1 - \rho)\bar{P}T}{TB - 1}, \quad (2)$$

respectively, where ρ is the fraction of total energy allocated to training. Note that the data symbol energy \mathcal{E}_s is obtained by uniformly allocating the remaining energy among the data symbols.

In the training phase, the receiver obtains the MMSE estimate \hat{h} which is a circularly symmetric, complex, Gaussian random variable with mean zero and variance $\frac{\gamma^2 \mathcal{E}_t}{\gamma \mathcal{E}_t + N_0}$, i.e., $\hat{h} \sim \mathcal{CN}\left(0, \frac{\gamma^2 \mathcal{E}_t}{\gamma \mathcal{E}_t + N_0}\right)$ [21]. Now, the channel fading coefficient h can be expressed as $h = \hat{h} + \tilde{h}$ where \tilde{h} is the estimate error and $\tilde{h} \sim \mathcal{CN}\left(0, \frac{\gamma N_0}{\gamma \mathcal{E}_t + N_0}\right)$. Consequently, in the data transmission phase, the channel input-output relation becomes

$$y[i] = \hat{h}[i]x[i] + \tilde{h}[i]x[i] + n[i] \quad i = 1, 2, \dots \quad (3)$$

Since finding the capacity of the channel in (3) is a difficult task¹, a capacity lower bound is generally obtained by considering the estimate error \tilde{h} as another source of Gaussian noise and treating $\tilde{h}[i]x[i] + n[i]$ as Gaussian distributed noise uncorrelated from the input. Now, the new noise variance is $\mathbb{E}\{|\tilde{h}[i]x[i] + n[i]|^2\} = \sigma_{\tilde{h}}^2 \mathcal{E}_s + N_0$ where $\sigma_{\tilde{h}}^2 = \mathbb{E}\{|\tilde{h}|^2\} = \frac{\gamma N_0}{\gamma \mathcal{E}_t + N_0}$ is the variance of the estimate error. Under these assumptions, a lower bound on the instantaneous capacity is given by [20], [21]

$$C_L = \frac{TB - 1}{T} \log_2 \left(1 + \frac{\mathcal{E}_s}{\sigma_{\tilde{h}}^2 \mathcal{E}_s + N_0} |\hat{h}|^2 \right) \quad (4)$$

$$= \frac{TB - 1}{T} \log_2 (1 + \text{SNR}_{\text{eff}} |w|^2) \quad \text{bits/s} \quad (5)$$

where effective SNR is

$$\text{SNR}_{\text{eff}} = \frac{\mathcal{E}_s \sigma_{\hat{h}}^2}{\sigma_{\tilde{h}}^2 \mathcal{E}_s + N_0}, \quad (6)$$

and $\sigma_{\hat{h}}^2 = \mathbb{E}\{|\hat{h}|^2\} = \frac{\gamma^2 \mathcal{E}_t}{\gamma \mathcal{E}_t + N_0}$ is the variance of estimate \hat{h} . Note that the expression in (5) is obtained by defining $\hat{h} = \sigma_{\hat{h}} w$ where w is a standard complex Gaussian random variable with zero mean and unit variance, i.e., $w \sim \mathcal{CN}(0, 1)$.

Since Gaussian is the worst uncorrelated noise [20], the above-mentioned assumptions lead to a pessimistic model and the rate expression in (5) is a lower bound to the capacity of the true channel (3). On the other hand, C_L is a good measure of the rates achieved in communication systems that operate as if the channel estimate were perfect (i.e., in systems where Gaussian codebooks designed for known channels are used, and scaled nearest neighbor decoding is employed at the receiver) [22].

¹In [21], the capacity of training-based transmissions under input peak power constraints is shown to be achieved by an SNR-dependent, discrete distribution with a finite number of mass points. In such cases, no closed-form expression for the capacity exists, and capacity values need to be obtained through numerical computations.

Henceforth, we base our analysis on C_L to understand the impact of the imperfect channel estimate. Since the transmitter is unaware of the channel conditions, it is assumed that information is transmitted at a fixed rate of r bits/s. When $r < C_L$, the channel is considered to be in the ON state and reliable communication is achieved at this rate. If, on the other hand, $r \geq C_L$, we assume that outage occurs. In this case, channel is in the OFF state and reliable communication at the rate of r bits/s cannot be attained. Hence, effective data rate is zero and information has to be resent. Fig. 1 depicts the two-state transmission model together with the transition probabilities. Under the assumption for independent realizations of blocks, it can be easily seen that the transition probabilities are given by

$$p_{11} = p_{21} = P\{r \geq C_L\} = P\{|w|^2 \leq \alpha\} \quad (7)$$

$$p_{22} = p_{12} = P\{r < C_L\} = P\{|w|^2 > \alpha\} \quad (8)$$

where

$$\alpha = \frac{2^{\frac{rT}{TB-1}} - 1}{\text{SNR}_{\text{eff}}}, \quad (9)$$

and $|w|^2$ is an exponential random variable with mean 1, and hence, $P\{|w|^2 > \alpha\} = e^{-\alpha}$.

III. PRELIMINARIES – EFFECTIVE CAPACITY AND SPECTRAL EFFICIENCY-BIT ENERGY TRADEOFF

In wireless communications, the instantaneous channel capacity varies randomly depending on the channel conditions. Hence, in addition to the source, the transmission rates for reliable communication are also time-varying. The time-varying channel capacity can be incorporated into the theory of effective bandwidth by regarding the channel service process as a time-varying source with negative rate and using the source multiplexing rule ([17, Example 9.2.2]). Using a similar approach, Wu and Negi in [4] defined the effective capacity as the maximum constant arrival rate that a given service process can support in order to guarantee a statistical QoS requirement specified by the QoS exponent θ ². If we define Q as the stationary queue length, then θ is the decay rate of the tail distribution of the queue length Q :

$$\lim_{q \rightarrow \infty} \frac{\log P(Q \geq q)}{q} = -\theta. \quad (10)$$

Therefore, for large q_{\max} , we have the following approximation for the buffer violation probability: $P(Q \geq q_{\max}) \approx e^{-\theta q_{\max}}$. Hence, while larger θ corresponds to more strict QoS constraints, smaller θ implies looser

²For time-varying arrival rates, effective capacity specifies the effective bandwidth of the arrival process that can be supported by the channel.

QoS guarantees. Similarly, if D denotes the steady-state delay experienced in the buffer, then $P(D \geq d_{\max}) \approx e^{-\theta \delta d_{\max}}$ for large d_{\max} , where δ is determined by the arrival and service processes [10].

The effective capacity is given by

$$-\frac{\Lambda(-\theta)}{\theta} = -\lim_{t \rightarrow \infty} \frac{1}{\theta t} \log_e \mathbb{E}\{e^{-\theta S[t]}\} \quad (11)$$

where $S[t] = \sum_{i=1}^t R[i]$ is the time-accumulated service process and $\{R[i], i = 1, 2, \dots\}$ denote the discrete-time stationary and ergodic stochastic service process. Note that in the model we consider, $R[i] = rT$ or 0 depending on the channel state being ON or OFF. In [17], it is shown that for such an ON-OFF model, we have

$$\frac{\Lambda(\theta)}{\theta} = \frac{1}{\theta} \log_e \left(\frac{1}{2} \left(p_{11} + p_{22} e^{\theta T r} + \sqrt{(p_{11} + p_{22} e^{\theta T r})^2 + 4(p_{11} + p_{22} - 1)e^{\theta T r}} \right) \right) \quad (12)$$

Note that $p_{11} + p_{22} = 1$ in our model. Then, for a given QoS delay constraint θ , the effective capacity normalized by the frame duration T and bandwidth B , or equivalently spectral efficiency in bits/s/Hz, becomes

$$R_E(\text{SNR}, \theta) = \max_{\substack{r \geq 0 \\ 0 \leq \rho \leq 1}} -\frac{1}{TB} \frac{\Lambda(-\theta)}{\theta} \quad \text{bits/s/Hz} \quad (13)$$

$$= \max_{\substack{r \geq 0 \\ 0 \leq \rho \leq 1}} -\frac{1}{\theta TB} \log_e (p_{11} + p_{22} e^{-\theta T r}) \quad (14)$$

$$= \max_{\substack{r \geq 0 \\ 0 \leq \rho \leq 1}} -\frac{1}{\theta TB} \log_e (1 - P(|w|^2 > \alpha)(1 - e^{-\theta T r})) \quad (15)$$

$$= -\frac{1}{\theta TB} \log_e (1 - P(|w|^2 > \alpha_{\text{opt}})(1 - e^{-\theta T r_{\text{opt}}})) \quad (16)$$

Note that R_E is obtained by optimizing both the fixed transmission rate r and the fraction of power allocated to training, ρ . In the optimization result (16), r_{opt} and α_{opt} are the optimal values of r and α , respectively.

The optimized r_{opt} can be found by solving

$$\frac{2^{\frac{T r}{TB-1}} T \log_e 2}{(TB-1) \text{SNR}_{\text{eff}}} (1 - e^{-\theta T r}) - \theta T e^{-\theta T r} = 0 \quad (17)$$

which is obtained from the first derivative of (15) over r .

It can easily be seen that

$$R_E(\text{SNR}, 0) = \lim_{\theta \rightarrow 0} R_E(\text{SNR}, \theta) = \max_{r \geq 0} \frac{r}{B} P \left\{ |w|^2 > \frac{2^{\frac{rT}{TB-1}} - 1}{\text{SNR}_{\text{eff}}} \right\}. \quad (18)$$

Hence, as the QoS requirements relax, the maximum constant arrival rate approaches the average transmission rate. On the other hand, for $\theta > 0$, $R_E < \frac{1}{B} \max_{r \geq 0} r P(|w|^2 > \alpha)$ in order to avoid violations of buffer constraints.

In this paper, we focus on the energy efficiency of wireless transmissions under the aforementioned statistical queueing constraints. Since energy efficient operation generally requires operation at low-SNR levels, our analysis throughout the paper is carried out in the low-SNR regime. In this regime, the tradeoff between the normalized effective capacity (i.e, spectral efficiency) R_E and bit energy $\frac{E_b}{N_0} = \frac{\text{SNR}}{R_E(\text{SNR})}$ is a key tradeoff in understanding the energy efficiency, and is characterized by the bit energy at zero spectral efficiency and wideband slope provided, respectively, by

$$\frac{E_b}{N_0} \Big|_{R=0} = \frac{1}{\dot{R}_E(0)} \text{ and } \mathcal{S}_0 = -\frac{2(\ddot{R}_E(0))^2}{\dot{R}_E(0)} \log_e 2 \quad (19)$$

where $\dot{R}_E(0)$ and $\ddot{R}_E(0)$ are the first and second derivatives with respect to SNR, respectively, of the function $R_E(\text{SNR})$ at zero SNR [1]. For the wideband regime detailed later, $\frac{E_b}{N_0} \Big|_{R=0} = \frac{E_b}{N_0 \min}$.

IV. LOW-POWER REGIME

Now, the normalized effective capacity is given by

$$R_E(\text{SNR}, \theta) = \max_{\substack{r \geq 0 \\ 0 \leq \rho \leq 1}} -\frac{1}{\theta TB} \log_e (1 - P(|w|^2 > \alpha)(1 - e^{-\theta Tr})) \text{ bits/s/Hz} \quad (20)$$

$$= -\frac{1}{\theta TB} \log_e (1 - P(|w|^2 > \alpha_{\text{opt}})(1 - e^{-\theta Tr_{\text{opt}}})) \text{ bits/s/Hz}. \quad (21)$$

Note that R_E is obtained by optimizing both the fixed transmission rate r and the fraction of power allocated to training, ρ . In the optimization result (21), r_{opt} and α_{opt} are the optimal values of r and α , respectively.

We first obtain the following result on the optimal value of ρ .

Theorem 1: At a given SNR level, the optimal fraction of power ρ_{opt} that solves (20) does not depend on the QoS exponent θ and the transmission rate r , and is given by

$$\rho_{\text{opt}} = \sqrt{\eta(\eta + 1)} - \eta \quad (22)$$

where $\eta = \frac{\gamma T B \text{SNR} + T B - 1}{\gamma T B (T B - 2) \text{SNR}}$ and $\text{SNR} = \frac{\bar{P}}{N_0 B}$.

Proof: From (20) and the definition of α in (9), we can easily see that for fixed r , the only term in (20) that depends on ρ is α . Moreover, α has this dependency through SNR_{eff} . Therefore, ρ_{opt} that maximizes the objective function in (20) can be found by minimizing α , or equivalently maximizing SNR_{eff} . Substituting the definitions in (2) and the expressions for σ_h^2 and σ_s^2 into (6), we have

$$\text{SNR}_{\text{eff}} = \frac{\mathcal{E}_s \sigma_h^2}{\sigma_h^2 \mathcal{E}_s + N_0} = \frac{\rho(1-\rho)\gamma^2 T^2 B^2 \text{SNR}^2}{\rho \gamma T B (T B - 2) \text{SNR} + \gamma T B \text{SNR} + T B - 1} \quad (23)$$

where $\text{SNR} = \frac{\bar{P}}{N_0 B}$. Evaluating the derivative of SNR_{eff} with respect to ρ and making it equal to zero leads to the expression in (22). Clearly, ρ_{opt} is independent of θ and r .

Above, we have implicitly assumed that the maximization is performed with respect to first ρ and then r . However, the result will not alter if the order of the maximization is changed. Note that the objective function in (20)

$$g(\text{SNR}_{\text{eff}}, r) = -\frac{1}{\theta T B} \log_e \left(1 - P \left(|w|^2 > \frac{2^{\frac{rT}{TB-1}} - 1}{\text{SNR}_{\text{eff}}} \right) (1 - e^{-\theta T r}) \right) \quad (24)$$

is a monotonically increasing function of SNR_{eff} for all r . It can be easily verified that maximization does not affect the monotonicity of g , and hence $\max_{r \geq 0} g(\text{SNR}_{\text{eff}}, r)$ is still a monotonically increasing function of SNR_{eff} . Therefore, in the outer maximization with respect to ρ , the choice of ρ that maximizes SNR_{eff} will also maximize $\max_{r \geq 0} g(\text{SNR}_{\text{eff}}, r)$, and the optimal value of ρ is again given by (22). \square

Fig. 2 plots ρ_{opt} , the optimal fraction of power allocated to training, as a function of SNR for different values of θ when $B = 10^7$ Hz. As predicted, ρ_{opt} is the same for all θ . Note that as $\text{SNR} \rightarrow 0$, we have $\eta \rightarrow \infty$ and $\rho_{\text{opt}} \rightarrow 1/2$, which is also observed in the figure. We further observe in Fig. 2 that ρ_{opt} decreases with increasing SNR. Moreover, as $\text{SNR} \rightarrow \infty$, we can find that $\eta \rightarrow \frac{1}{T B - 2}$ and hence $\rho_{\text{opt}} \rightarrow \sqrt{\frac{1}{T B - 2} \left(\frac{1}{T B - 2} + 1 \right) - \frac{1}{T B - 2}}$. In the figure, we assume $T = 2$ ms, and therefore $T B = 2 \times 10^4$ and $\rho_{\text{opt}} \rightarrow 0.007$.

With the optimal value of ρ given in Theorem 1, we can now express the normalized effective capacity as

$$\mathcal{R}_E(\text{SNR}, \theta) = \max_{r \geq 0} -\frac{1}{\theta T B} \log_e \left(1 - P \left(|w|^2 > \frac{2^{\frac{rT}{TB-1}} - 1}{\text{SNR}_{\text{eff, opt}}} \right) (1 - e^{-\theta T r}) \right) \quad (25)$$

where

$$\text{SNR}_{\text{eff, opt}} = \frac{\phi(\text{SNR}) \text{SNR}^2}{\psi(\text{SNR}) \text{SNR} + T B - 1}, \quad (26)$$

and

$$\phi(\text{SNR}) = \rho_{\text{opt}}(1 - \rho_{\text{opt}})\gamma^2 T^2 B^2, \text{ and } \psi(\text{SNR}) = (1 + (TB - 2)\rho_{\text{opt}})\gamma TB. \quad (27)$$

With these notations, we obtain the following result that shows us that operation at very low power levels is extremely energy inefficient and should be avoided.

Theorem 2: In the case of imperfectly-known channel, the bit energy increases without bound as the average power \bar{P} and hence SNR vanishes, i.e.,

$$\left. \frac{E_b}{N_0} \right|_{R=0} = \lim_{\text{SNR} \rightarrow 0} \frac{E_b}{N_0} = \lim_{\text{SNR} \rightarrow 0} \frac{\text{SNR}}{R_E(\text{SNR})} = \frac{1}{\dot{R}_E(0)} = \infty. \quad (28)$$

Proof: Essentially, R_E in (25) can be seen to be a function of $\text{SNR}_{\text{eff,opt}}$. Compared with the discussion in [15, Appendix B], we can find that the difference is that we have $\alpha = \frac{2^{\frac{rT}{TB-1}} - 1}{\text{SNR}_{\text{eff,opt}}}$ in (25). Then, using similar techniques, we can easily obtain the following first-order low-SNR expansion:

$$R_E(\text{SNR}) = \frac{aP\{|w|^2 > \alpha_{\text{opt}}^*\}}{B} \text{SNR}_{\text{eff,opt}} + o(\text{SNR}_{\text{eff,opt}}) \quad (29)$$

$$= \frac{TB - 1}{TB} \frac{\alpha_{\text{opt}}^* P\{|w|^2 > \alpha_{\text{opt}}^*\}}{\log_e 2} \text{SNR}_{\text{eff,opt}} + o(\text{SNR}_{\text{eff,opt}}) \quad (30)$$

where $\alpha_{\text{opt}}^* = \lim_{\text{SNR} \rightarrow 0} \alpha_{\text{opt}}$. Note that as $\text{SNR} \rightarrow 0$, $\eta \rightarrow \infty$, $\rho_{\text{opt}} \rightarrow 1/2$, and hence $\phi(\text{SNR}) \rightarrow 1/4\gamma^2 T^2 B^2$. Then, we have

$$\text{SNR}_{\text{eff,opt}} = \frac{\gamma^2 T^2 B^2}{4(TB - 1)} \text{SNR}^2 + o(\text{SNR}^2). \quad (31)$$

Hence, $\text{SNR}_{\text{eff,opt}}$ scales as SNR^2 as SNR diminishes to zero, which implies from (30) that R_E scales as SNR^2 as well. Therefore, the first derivative of R_E with respect to SNR is zero at $\text{SNR} = 0$, i.e., $\dot{R}_E(0) = 0$, leading to the result that $\lim_{\text{SNR} \rightarrow 0} \frac{E_b}{N_0} = \infty$. \square

Remark: Theorem 2 shows that the $\left. \frac{E_b}{N_0} \right|_{R_E=0}$ for any $\theta \geq 0$ goes to infinity. This is in consistent with previous results for unknown channels without queueing constraints [21]. But as will be seen in the numerical results, bit energy to achieve a certain level of spectral efficiency increases with θ in this case.

With the analytical result on the energy efficiency–spectral efficiency tradeoff, we now try to prove the theoretical findings through numerical computations. Fig. 3 plots the spectral efficiency vs. bit energy for $\theta = \{1, 0.1, 0.01, 0.001\}$ when $B = 10^5$ Hz in Rayleigh channel with $\mathbb{E}\{|h|^2\} = \gamma = 1$. We immediately notice a different behavior as $\text{SNR} \rightarrow 0$ and hence the spectral efficiency decreases. As predicted by the result of Theorem 2, the bit energy increases without bound as $R_E \rightarrow 0$ in all cases. The minimum bit

energy is achieved at a nonzero spectral efficiency below which one should avoid operating as it only increases the energy requirements. Since the closed form expression for minimum bit energy is untractable, to give an idea of what is happening at minimum bit energy, we plot $\frac{E_b}{N_0}$ as a function of SNR for different bandwidth levels assuming $\theta = 0.01$ in Fig. 4. As predicted before, we again observe that the minimum bit energy is attained at a nonzero SNR value below which $\frac{E_b}{N_0}$ requirements start increasing. Furthermore, we see that as the bandwidth increases, the minimum bit energy tends to decrease and is achieved at a lower SNR level. Finally, we plot in Fig. 5 the minimum bit energy as a function of the bandwidth, B . We note that increasing B generally decreases $\frac{E_b}{N_0 \min}$ when $\theta = 0$. However, for the cases in which $\theta > 0$ and there exist QoS constraints, there is no improvement as B is increased above a certain value. Thus, analysis in the wideband regime where $B \rightarrow \infty$ will provide us some insightful results.

V. WIDEBAND REGIME

In this section, we consider the wideband regime in which the bandwidth is large. We assume that the average power \bar{P} is kept constant. Note that as the bandwidth B increases, $\text{SNR} = \frac{\bar{P}}{N_0 B}$ approaches zero and we operate in the low-SNR regime.

Following the approach generally employed in the information-theoretic analyses, we assume that the wideband channel is decomposed into N parallel subchannels. We further assume that each subchannel has a bandwidth that is equal to the coherence bandwidth, B_c . Therefore, independent flat-fading is experienced in each subchannel, and we have $B = NB_c$. Similar to (1), the input-output relation in the k^{th} subchannel can be written as

$$y_k[i] = h_k[i]x_k[i] + n_k[i] \quad i = 1, 2, \dots \quad \text{and} \quad k = 1, 2, \dots, N. \quad (32)$$

The fading coefficients $\{h_k\}_{k=1}^N$ in different subchannels are assumed to be independent with $\mathbb{E}\{|h_k|^2\} = \gamma_k$. The signal-to-noise ratio in the k^{th} subchannel is $\text{SNR}_k = \frac{\bar{P}_k}{N_0 B_c}$ where \bar{P}_k denotes the power allocated to the k^{th} subchannel and we have $\sum_{k=1}^N \bar{P}_k = \bar{P}$. Over each subchannel, the same transmission strategy as described in Section II is employed. Therefore, the transmitter, not knowing the fading coefficients of the subchannels, sends the data over each subchannel at the fixed rate of r . Now, we can find that $C_{L,k}$ for each subchannel is given by $\frac{TB_c-1}{T} \log_2(1 + \text{SNR}_{\text{eff},k}|w|^2)$ bits/s, in which

$$\text{SNR}_{\text{eff},k} = \frac{\mathcal{E}_{s,k} \sigma_{h_k}^2}{\sigma_{h_k}^2 \mathcal{E}_{s,k} + N_0} \quad (33)$$

where $\mathcal{E}_{s,k} = \frac{(1-\rho_k)T\bar{P}_k}{TB_c-1}$, $\mathcal{E}_{t,k} = \rho_k T \bar{P}_k$, $\sigma_{h_k}^2 = \frac{\gamma_k N_0}{\gamma_k \mathcal{E}_{t,k} + N_0}$ and $\sigma_{h_k}^2 = \frac{\gamma_k^2 \mathcal{E}_{t,k}}{\gamma_k \mathcal{E}_{t,k} + N_0}$. Similarly, if $r < C_{L,k}$, then

transmission over the k^{th} subchannel is successful. Otherwise, retransmission is required. Hence, we have an ON-OFF state model for each subchannel. On the other hand, for the transmission over N subchannels, we have a state-transition model with $N + 1$ states because we have overall the following $N + 1$ possible total transmission rates: $\{0, rT, 2rT, \dots, NrT\}$. For instance, if all N subchannels are in the OFF state simultaneously, the total rate is zero. If j out of N subchannels are in the ON state, then the rate is jrT .

Now, assume that the states are enumerated in the increasing of order of the total transmission rates supported by them. Hence, in state $j \in \{1, \dots, N + 1\}$, the transmission rate is $(j - 1)rT$. The transition probability from state $i \in \{1, \dots, N + 1\}$ to state $j \in \{1, \dots, N + 1\}$ is given by

$$p_{i,j} = p_j = P\{(j - 1) \text{ subchannels out of } N \text{ subchannels are in the ON state}\} \quad (34)$$

$$= \sum_{\mathcal{I}_{j-1} \subset \{1, \dots, N\}} \left(\prod_{k \in \mathcal{I}_{j-1}} P\{|w|^2 > \alpha_k\} \prod_{k \in \mathcal{I}_{j-1}^c} (1 - P\{|w|^2 > \alpha_k\}) \right) \quad (35)$$

where \mathcal{I}_{j-1} denotes a subset of the index set $\{1, \dots, N\}$ with $j - 1$ elements. The summation in (35) is over all such subsets. Moreover, in (35), \mathcal{I}_{j-1}^c denotes the complement of the set \mathcal{I}_{j-1} , and $\alpha_k = \frac{2^{\frac{rT}{TB_c-1}} - 1}{\text{SNR}_{\text{eff},k}}$. Note in the above formulation that the transition probabilities, $p_{i,j}$, do not depend on the initial state i due to the block-fading assumption. If, in addition to being independent, the fading coefficients h_k in different subchannels are identically distributed, and hence $\{\gamma_k\}_{k=1}^N$ are the same, then $p_{i,j}$ in (35) simplifies and becomes a binomial probability:

$$p_{i,j} = p_j = \binom{N}{j-1} (P\{|w|^2 > \alpha\})^{j-1} (1 - P\{|w|^2 > \alpha\})^{N-j+1}. \quad (36)$$

Note that if the fading coefficients are i.i.d., the total power should be uniformly distributed over the subchannels. Hence, in this case, we have $\bar{P}_k = \frac{\bar{P}}{N}$ and therefore $\text{SNR}_k = \frac{\bar{P}_k}{N_0 B_c} = \frac{\bar{P}/N}{N_0 B/N} = \frac{\bar{P}}{N_0 B} = \text{SNR}$ which is equal to the original SNR used in (22). Since $\{\text{SNR}_{\text{eff},k}\}_{k=1}^N$ are the same in (33), we have the same $\alpha = \frac{2^{\frac{rT}{TB_c-1}} - 1}{\text{SNR}_{\text{eff},k}}$ for each subchannel.

The effective capacity of this wideband channel model is given by the following result.

Theorem 3: For the wideband channel with N parallel noninteracting subchannels each with bandwidth B_c and independent flat fading, the normalized effective capacity in bits/s/Hz is

$$\mathbf{R}_E(\text{SNR}, \theta) = \max_{r \geq 0} \left\{ -\frac{1}{\theta TB} \log_e \left(\sum_{j=1}^{N+1} p_j e^{-\theta(j-1)rT} \right) \right\} \quad (37)$$

where p_j is given in (35). If $\{h_k\}_{k=1}^N$ are identically distributed, then the normalized effective capacity

expression simplifies to

$$R_E(\text{SNR}, \theta) = \max_{r \geq 0} \left\{ -\frac{1}{\theta T B_c} \log_e \left(1 - P\{|w|^2 > \alpha\} (1 - e^{-\theta T r}) \right) \right\}. \quad (38)$$

where $\alpha = \frac{2^{rT} - 1}{\text{SNR}_{\text{eff}}}$ and $\text{SNR}_{\text{eff}} = \frac{\rho(1-\rho)\gamma^2 T^2 B_c^2 \text{SNR}^2}{\rho\gamma T B_c (T B_c - 2) \text{SNR} + \gamma T B_c \text{SNR} + T B_c - 1}$, in which $\text{SNR} = \frac{\bar{P}}{N_0 B} = \frac{\bar{P}}{N N_0 B_c}$.

Proof: See Appendix A.

Theorem 3 shows that the effective capacity of a wideband channel with N subchannels each with i.i.d. flat fading has an expression similar to that in (21), which provides the effective capacity of a single channel experiencing flat fading. The only difference between (21) and (38) is that B is replaced in (38) by B_c , which is the bandwidth of each subchannel.

In this section, we consider the wideband regime in which the overall bandwidth of the system, B , is large. In particular, we analyze the performance in the scenario of sparse multipath fading. Motivated by the recent measurement studies in the ultrawideband regime, the authors in [23] and [24] considered sparse multipath fading channels and analyzed the performance under channel uncertainty, employing the Shannon capacity formulation as the performance metric. In particular, [23] and [24] noted that the number of independent resolvable paths in sparse multipath channels increase at most sublinearly with the bandwidth, which in turn causes the coherence bandwidth B_c to increase with increasing bandwidth. To characterize the performance of sparse fading channels in the wideband regime, we assume in this section that $B_c \rightarrow \infty$ as $B \rightarrow \infty$. We further assume that the the number of subchannels N remains bounded and the degrees of freedom are limited. For instance, this case arises if the number of resolvable paths are bounded even at infinite bandwidth. Such a scenario is considered in [25] where the capacity and mutual information are characterized under channel uncertainty in the wideband regime with bounded number of paths.

The following result provides the expressions for the bit energy at zero spectral efficiency and the wideband slope, and characterize the spectral efficiency-bit energy tradeoff in the wideband regime.

Theorem 4: In the wideband regime, the bit energy at zero spectral efficiency and wideband slope are given by

$$\left. \frac{E_b}{N_0} \right|_{\min} = \frac{-\delta \log_e 2}{\log_e \xi} \quad \text{and} \quad (39)$$

$$\mathcal{S}_0 = \frac{\xi \log_e^2 \xi \log_e 2}{\theta T \alpha_{\text{opt}}^* (1 - \xi) \left(\frac{1}{T} \left(\sqrt{1 + \frac{\gamma \bar{P} T}{N N_0}} - 1 \right) + \frac{\varphi \alpha_{\text{opt}}^*}{2} \right)}, \quad (40)$$

respectively, where $\delta = \frac{\theta T \bar{P}}{NN_0 \log_e 2}$, $\xi = 1 - e^{-\alpha_{\text{opt}}^*} (1 - e^{-\frac{\theta T \varphi \alpha_{\text{opt}}^*}{\log_e 2}})$, and $\varphi = \frac{\gamma \bar{P}}{NN_0} \left(\sqrt{1 + \frac{NN_0}{\gamma PT}} - \sqrt{\frac{NN_0}{\gamma PT}} \right)^2$. α_{opt}^* is defined as $\alpha_{\text{opt}}^* = \lim_{\zeta \rightarrow 0} \alpha_{\text{opt}}$ and α_{opt}^* satisfies

$$\alpha_{\text{opt}}^* = \frac{\log_e 2}{\theta T \varphi} \log_e \left(1 + \frac{\theta T \varphi}{\log_e 2} \right). \quad (41)$$

Proof: See Appendix B.

We note that the minimum bit energy in the wideband regime is achieved as $B \rightarrow \infty$ and hence as $\text{SNR} \rightarrow 0$. This is in stark contrast to the results in the low-power regime in which the bit energy requirements grow without bound as \bar{P} and SNR vanishes.

Remark: Theorem 4, through the minimum bit energy and wideband slope expressions, quantifies the bit energy requirements in the wideband regime when the system is operating subject to both statistical QoS constraints specified by θ and channel uncertainty. Note that both $\left. \frac{E_b}{N_0} \right|_{\min}$ and \mathcal{S}_0 depend on θ through δ and ξ . As will be observed in the numerical results, $\left. \frac{E_b}{N_0} \right|_{\min}$ and the bit energy requirements at nonzero spectral efficiency values generally increase with increasing θ . Moreover, when compared with the results in Section IV, it will be seen that sparse multipath fading and having a bounded number of subchannels incur energy penalty no matter there is QoS constraints or not ($\theta = 0$), which is in stark contrast with previous results when there is perfect CSI at the receiver [15].

Having quantified the minimum bit energy and wideband slope through the analytical expression, we seek to find support through numerical computations. Fig. 6 plots the spectral efficiency–bit energy curve in the Rayleigh channel for different θ values. In the figure, we assume that $\bar{P}/(NN_0) = 10^4$. As predicted, the minimum bit energies are obtained as SNR and hence the spectral efficiency approach zero. $\left. \frac{E_b}{N_0} \right|_{\min}$ are computed to be equal to $\{4.6776, 4.7029, 4.9177, 6.3828, 10.8333\}$ dB for $\theta = \{0, 0.001, 0.01, 0.1, 1\}$, respectively. Moreover, the wideband slopes are $\mathcal{S}_0 = \{0.4720, 0.4749, 0.4978, 0.6151, 0.6061\}$ for the same set of θ values. As can also be seen in the result of Theorem 4, the minimum bit energy and wideband slope in general depend on θ . In Fig. 6, we note that the bit energy requirements (including the minimum bit energy) increase with increasing θ , illustrating the energy costs of stringent queueing constraints. Finally, in this paper, we have considered fixed-rate/fixed-power transmissions over imperfectly-known channels. In Fig. 7, we compare the performance of this system with those in which the channel is perfectly-known and fixed- or variable-rate transmission is employed. The latter models have been studied in [14] and [15]. This figure demonstrates the energy costs of not knowing the channel and sending the information at fixed-rate.

In previous discussion, the number of subchannels are implicitly assumed to be bounded. Meanwhile, the

discussion in Section IV can be considered as the rich multipath fading channels in which the number of subchannels increases linearly with bandwidth. A scenario in between these two cases is the one in which the number of subchannels N increases but only sublinearly with increasing bandwidth. As N increases, each subchannel is allocated less power and operate in the low-power regime. At the same time, since N increases sublinearly with B , the coherence bandwidth $B_c = B/N$ also increases. Therefore, the minimum bit energy and wideband slope expressions for this scenario can be obtained by letting N in the results of Theorem 4 go to infinity.

Corollary 1: In the wideband regime, if the number of subchannels N increases sublinearly with B , then the minimum bit energy and wideband slope are given by

$$\left. \frac{E_b}{N_0} \right|_{R_E=0} = \infty \quad \text{and} \quad \mathcal{S}_0 = 0 \quad (42)$$

Numerical result is illustrated in Fig. 8. Although the immediate theoretical result is similar to that in Theorem 2, compared with Fig.3, we see that although the same minimum bit energy is attained for all $\theta \geq 0$, approaching this minimum energy level is extremely slow and demanding when $\theta > 0$.

VI. CONCLUSION

In this paper, we have analyzed the energy efficiency of fixed-rate wireless transmissions for the communication scenario in which queueing constraints are present and the channel coefficients are estimated imperfectly by the receiver with the aid of training symbols. We have considered the effective capacity as a measure of the maximum throughput under statistical QoS constraints. We have identified the optimal fraction of power allocated to training and shown that this optimal fraction do not depend on the QoS exponent θ and the transmission rate. In particular, we have investigated the spectral efficiency–bit energy tradeoff in the low-power and wideband regimes. In the low-power regime, we have shown that the bit energy increases without bound as power diminishes. The minimum bit energy is achieved at a certain non-zero power level below which operation should be avoided. Although the minimum bit energy cannot be specified in closed form expression, we have found that as QoS constraints become more stringent, the minimum bit energy increases. In the wideband regime, we have shown that the bit energy required at zero spectral efficiency (or equivalently at infinite bandwidth) is the minimum bit energy. We have noted that the minimum bit energy and wideband slope in general depend on the QoS exponent θ . As the QoS constraints become more stringent and hence θ is increased, we have observed in the numerical results that the required minimum bit energy increases. Overall, we have specified the bit energy requirement in the low-power regime, quantified

the increased energy requirements in the presence of QoS constraints in wideband regime, and identified the impact upon the energy efficiency of multipath sparsity and richness in the wideband regime.

APPENDIX

A. Proof of Theorem 3

In [17, Chap. 7, Example 7.2.7], it is shown for Markov modulated processes that $\frac{\Lambda(\theta)}{\theta} = \frac{1}{\theta} \log_e sp(\Phi(\theta)\mathbf{P})$ where $sp(\Phi(\theta)\mathbf{P})$ is the spectral radius (i.e., the maximum of the absolute values of the eigenvalues) of the matrix $\Phi(\theta)\mathbf{P}$, \mathbf{P} is the transition matrix of the underlying Markov process, and $\Phi(\theta)$ is a diagonal matrix whose j^{th} component, $\phi_j(\theta)$, is the moment generating function of the random process $y_j(t)$ given in this state. Hence, we have $\phi_j(\theta) = E\{e^{\theta y_j(t)}\}$.

The transmission model described for the wideband channel with N subchannels is a Markov-modulated process where the underlying Markov process has $N + 1$ states with the transition probabilities given in (35). Hence, the transition matrix is

$$\mathbf{P} = \begin{bmatrix} p_{1,1} & p_{1,2} & \cdot & \cdot & p_{1,N+1} \\ \cdot & & & & \cdot \\ \cdot & & & & \cdot \\ p_{N+1,1} & p_{N+1,2} & \cdot & \cdot & p_{N+1,N+1} \end{bmatrix} = \begin{bmatrix} p_1 & p_2 & \cdot & \cdot & p_{N+1} \\ \cdot & & & & \cdot \\ \cdot & & & & \cdot \\ p_1 & p_2 & \cdot & \cdot & p_{N+1} \end{bmatrix}. \quad (43)$$

Note that the rows of \mathbf{P} are identical due to the fact that the transition probabilities do not depend on the initial state. In each state, the transmission rate is non-random and fixed. Recall that in state j , the transmission rate is equal to $(j - 1)rT$. The moment generating function of this deterministic process is $\phi_j(\theta) = E\{e^{\theta(j-1)rT}\} = e^{\theta(j-1)rT}$. Therefore, we have

$$\Phi(\theta)\mathbf{P} = \underbrace{\begin{bmatrix} 1 & 0 & \cdot & \cdot & 0 \\ 0 & e^{\theta rT} & 0 & \cdot & 0 \\ \cdot & & & & \cdot \\ 0 & 0 & \cdot & 0 & e^{\theta N rT} \end{bmatrix}}_{\Phi(\theta)} \underbrace{\begin{bmatrix} p_1 & p_2 & \cdot & \cdot & p_{N+1} \\ \cdot & & & & \cdot \\ \cdot & & & & \cdot \\ p_1 & p_2 & \cdot & \cdot & p_{N+1} \end{bmatrix}}_{\mathbf{P}} = \begin{bmatrix} p_1 & p_2 & \cdot & \cdot & p_{N+1} \\ p_1 e^{\theta rT} & p_2 e^{\theta rT} & \cdot & \cdot & p_{N+1} e^{\theta rT} \\ \cdot & & & & \cdot \\ p_1 e^{\theta N rT} & p_2 e^{\theta N rT} & \cdot & \cdot & p_{N+1} e^{\theta N rT} \end{bmatrix}. \quad (44)$$

Note that the rows of $\Phi(\theta)\mathbf{P}$ are multiples of each other, and hence $\Phi(\theta)\mathbf{P}$ is a matrix of unit rank. This leads to the conclusion that $sp(\Phi(\theta)\mathbf{P}) = \text{trace}(\Phi(\theta)\mathbf{P}) = \sum_{j=1}^{N+1} p_j e^{\theta(j-1)rT}$. Therefore, for the wideband channel in consideration, we have $\frac{\Lambda(\theta)}{\theta} = \frac{1}{\theta} \log_e sp(\Phi(\theta)\mathbf{P}) = \frac{1}{\theta} \log_e \left(\sum_{j=1}^{N+1} p_j e^{\theta(j-1)rT} \right)$. Applying the definition $R_E(\text{SNR}, \theta) = \frac{1}{TB} \max_{r \geq 0} \left\{ -\frac{\Lambda(-\theta)}{\theta} \right\}$, we immediately obtain (37).

Assume now that $\{z_k\}_{k=1}^N$ are identically distributed and therefore p_j is in the binomial form given in

(36). Then, we can easily see that

$$\sum_{j=1}^{N+1} p_j e^{\theta(j-1)rT} = \sum_{j=1}^{N+1} \binom{N}{j-1} (P\{|w|^2 > \alpha\})^{j-1} (1 - P\{|w|^2 > \alpha\})^{N-j+1} e^{\theta(j-1)rT} \quad (45)$$

$$= \sum_{i=0}^N \binom{N}{i} (P\{|w|^2 > \alpha\} e^{\theta rT})^i (1 - P\{|w|^2 > \alpha\})^{N-i} \quad (46)$$

$$= (1 - P\{|w|^2 > \alpha\} + P\{|w|^2 > \alpha\} e^{\theta rT})^N \quad (47)$$

$$= (1 - P\{|w|^2 > \alpha\} (1 - e^{\theta rT}))^N. \quad (48)$$

Above, (46) is obtained by applying a change of variables with $i = j - 1$ and combining the second and fourth terms in the summation in (45) to write $(P\{|w|^2 > \alpha\} e^{\theta rT})^i$. (47) follows from the Binomial Theorem. Then, the expression in (38) is readily obtained by noting that $\frac{B}{N} = B_c$. \square

B. Proof of Theorem 4

We first derive the following result for optimal fraction of power on training expressed in (22)

$$\rho_{\text{opt}} = \rho_{\text{opt}}^* + \rho_{\text{opt}}^{\cdot}(0)\zeta + o(\zeta) \quad (49)$$

where ρ_{opt}^* is a real value achieved as $\zeta \rightarrow 0$, and $\rho_{\text{opt}}^{\cdot}(0)$ is the first derivative of ρ_{opt} evaluated at $\zeta = 0$.

We have

$$\rho_{\text{opt}}^* = \sqrt{\frac{NN_0}{\gamma\bar{P}T} \left(1 + \frac{NN_0}{\gamma\bar{P}T}\right)} - \frac{NN_0}{\gamma\bar{P}T} \quad (50)$$

and

$$\rho_{\text{opt}}^{\cdot}(0) = \frac{1}{2T} \sqrt{1 + \frac{\gamma\bar{P}T}{NN_0}} \left(\sqrt{1 + \frac{NN_0}{\gamma\bar{P}T}} - \sqrt{\frac{NN_0}{\gamma\bar{P}T}} \right)^2. \quad (51)$$

Furthermore, $\text{SNR}_{\text{eff,opt}}$ defined below equation (25) can be simplified to

$$\text{SNR}_{\text{eff,opt}} = \varphi\zeta + \omega\zeta^2 + o(\zeta^2) \quad (52)$$

where

$$\varphi = \frac{\rho_{\text{opt}}^* (1 - \rho_{\text{opt}}^*) \frac{\gamma^2 \bar{P}^2 T}{(NN_0)^2}}{1 + \frac{\rho_{\text{opt}}^* \gamma \bar{P} T}{NN_0}} = \frac{\gamma \bar{P}}{NN_0} \left(\sqrt{1 + \frac{NN_0}{\gamma \bar{P} T}} - \sqrt{\frac{NN_0}{\gamma \bar{P} T}} \right)^2 \quad (53)$$

and

$$\begin{aligned}\omega &= \frac{\frac{\gamma^2 P^2 T}{NN_0^2}}{1 + \rho_{\text{opt}}^* \frac{\gamma \bar{P} T}{NN_0}} \left(\rho_{\text{opt}}(0)(1 - 2\rho_{\text{opt}}^*) - \frac{(1 - 2\rho_{\text{opt}}^*) \frac{\gamma \bar{P}}{NN_0} + \rho_{\text{opt}}(0) \frac{\gamma \bar{P} T}{NN_0} - \frac{1}{T}}{1 + \frac{\rho_{\text{opt}}^* \gamma \bar{P} T}{NN_0}} \rho_{\text{opt}}^*(1 - \rho_{\text{opt}}^*) \right) \\ &= -\frac{\gamma \bar{P}}{NN_0 T} \left(\sqrt{1 + \frac{NN_0}{\gamma \bar{P} T}} - \sqrt{\frac{NN_0}{\gamma \bar{P} T}} \right)^2 \left(\sqrt{1 + \frac{\gamma \bar{P} T}{NN_0}} - 2 \right).\end{aligned}\quad (54)$$

Assume that the Taylor series expansion of r_{opt} with respect to small ζ is

$$r_{\text{opt}} = r_{\text{opt}}^* + \dot{r}_{\text{opt}}(0)\zeta + o(\zeta) \quad (55)$$

where $r_{\text{opt}}^* = \lim_{\zeta \rightarrow 0} r_{\text{opt}}$ and $\dot{r}_{\text{opt}}(0)$ is the first derivative with respect to ζ of r_{opt} evaluated at $\zeta = 0$. From (9), we can find that

$$\alpha_{\text{opt}} = \frac{2^{\frac{r_{\text{opt}} \zeta}{1 - \zeta/T}} - 1}{\text{SNR}_{\text{eff, opt}}} \quad (56)$$

$$\begin{aligned}&= \frac{r_{\text{opt}}^* \log_e 2 + \left[\left(\frac{r_{\text{opt}}^*}{T} + \dot{r}_{\text{opt}}(0) \right) \log_e 2 + \frac{(r_{\text{opt}}^* \log_e 2)^2}{2} \right] \zeta + o(\zeta)}{\varphi + \omega \zeta + o(\zeta)} \\ &= \frac{r_{\text{opt}}^* \log_e 2}{\varphi} + \left(\frac{\dot{r}_{\text{opt}}(0) \log_e 2}{\varphi} + \frac{r_{\text{opt}}^* \log_e 2}{\varphi} \left(\frac{1}{T} - \frac{\omega}{\varphi} \right) + \frac{(r_{\text{opt}}^* \log_e 2)^2}{2\varphi} \right) \zeta + o(\zeta)\end{aligned}\quad (57)$$

from which we have as $\zeta \rightarrow 0$ that

$$\alpha_{\text{opt}}^* = \frac{r_{\text{opt}}^* \log_e 2}{\varphi} \quad (58)$$

and that

$$\dot{\alpha}_{\text{opt}}(0) = \frac{\dot{r}_{\text{opt}}(0) \log_e 2}{\varphi} + \frac{r_{\text{opt}}^* \log_e 2}{\varphi} \left(\frac{1}{T} - \frac{\omega}{\varphi} \right) + \frac{(r_{\text{opt}}^* \log_e 2)^2}{2\varphi} \quad (59)$$

where $\dot{\alpha}_{\text{opt}}(0)$ is the first derivative with respect to ζ of α_{opt} evaluated at $\zeta = 0$. According to (58), $r_{\text{opt}}^* = \frac{\varphi \alpha_{\text{opt}}^*}{\log_e 2}$.

Combining with (52) and (58), we can obtain from (17)³ as $\zeta \rightarrow 0$

$$\frac{\log_e 2}{\varphi} \left(1 - e^{-\frac{\theta T \varphi \alpha_{\text{opt}}^*}{\log_e 2}} \right) - \theta T e^{-\theta T r_{\text{opt}}^*} = 0 \quad (60)$$

from which we get

$$\alpha_{\text{opt}}^* = \frac{\log_e 2}{\theta T \varphi} \log_e \left(1 + \frac{\theta T \varphi}{\log_e 2} \right). \quad (61)$$

Since $\frac{E_b}{NN_0} = \frac{\bar{P}}{\text{R}_E(\zeta)}$, the result that $\left. \frac{E_b}{NN_0} \right|_{\text{R}_E=0} = \frac{E_b}{NN_0}_{\text{min}}$ follows from the fact that $\text{R}_E(\zeta)/\zeta$ monotonically

³ B is replaced by B_c here according to (38).

decreases with increasing ζ , and hence achieves its maximum as $\zeta \rightarrow 0$. We now have

$$\frac{E_b}{NN_{0\min}} = \lim_{\zeta \rightarrow 0} \frac{\frac{\bar{P}}{NN_0} \zeta}{R_E(\zeta)} = \frac{-\frac{\theta T \bar{P}}{NN_0}}{\log_e (1 - P\{|w|^2 \geq \alpha_{\text{opt}}^*\})(1 - e^{-\theta T r_{\text{opt}}^*})} \quad (62)$$

$$= \frac{-\delta \log_e 2}{\log_e \xi} = \frac{\frac{\bar{P}}{NN_0}}{\dot{R}_E(0)} \quad (63)$$

where $\dot{R}_E(0)$ is the derivative of R_E with respect to ζ at $\zeta = 0$, $\delta = \frac{\theta T \bar{P}}{NN_0 \log_e 2}$, and $\xi = 1 - P\{|w|^2 \geq \alpha_{\text{opt}}^*\}(1 - e^{-\frac{\theta T \varphi \alpha_{\text{opt}}^*}{\log_e 2}})$. Obviously, (63) provides (39).

Note that the second derivative $\ddot{R}_E(0)$, required in the computation of the wideband slope \mathcal{S}_0 , can be obtained from

$$\begin{aligned} \ddot{R}_E(0) &= \lim_{\zeta \rightarrow 0} 2 \frac{R_E(\zeta) - \dot{R}_E(0)\zeta}{\zeta^2} \\ &= \lim_{\zeta \rightarrow 0} 2 \frac{1}{\zeta} \left(-\frac{1}{\theta T} \log_e (1 - P\{|w|^2 \geq \alpha_{\text{opt}}\})(1 - e^{-\theta T r_{\text{opt}}}) + \frac{1}{\theta T} \log_e (1 - P\{|w|^2 \geq \alpha_{\text{opt}}^*\})(1 - e^{-\theta T r_{\text{opt}}^*}) \right) \\ &= \lim_{\zeta \rightarrow 0} -\frac{2e^{-\alpha_{\text{opt}}}}{\theta T (1 - P\{|w|^2 \geq \alpha_{\text{opt}}\})(1 - e^{-\theta T r_{\text{opt}}})} (\dot{\alpha}_{\text{opt}}(\zeta)(1 - e^{-\theta T r_{\text{opt}}}) - \theta T e^{-\theta T r_{\text{opt}}} \dot{r}_{\text{opt}}(\zeta)) \end{aligned} \quad (64)$$

$$= -\frac{2e^{-\alpha_{\text{opt}}^*}}{\theta T (1 - P\{|w|^2 \geq \alpha_{\text{opt}}^*\})(1 - e^{-\theta T r_{\text{opt}}^*})} (\dot{\alpha}_{\text{opt}}(0)(1 - e^{-\theta T r_{\text{opt}}^*}) - \theta T e^{-\theta T r_{\text{opt}}^*} \dot{r}_{\text{opt}}(0)) \quad (65)$$

where $r_{\text{opt}}^* = \frac{\bar{P} \alpha_{\text{opt}}^*}{NN_0 \log_e 2}$. Above, (64) and (65) follow by using L'Hospital's Rule and applying Leibniz Integral Rule.

Meanwhile, substituting (60) and (59) into (65) gives us

$$\begin{aligned} \ddot{R}_E(0) &= -\frac{2e^{-\alpha_{\text{opt}}^*}}{\theta T (1 - P\{|w|^2 \geq \alpha_{\text{opt}}^*\})(1 - e^{-\theta T r_{\text{opt}}^*})} \alpha_{\text{opt}}^* (1 - e^{-\theta T r_{\text{opt}}^*}) \left(\frac{1}{T} - \frac{\omega}{\varphi} + \frac{\varphi \alpha_{\text{opt}}^*}{2} \right) \\ &= -\frac{2(1 - \xi) \alpha_{\text{opt}}^*}{\theta T \xi} \left(\frac{1}{T} - \frac{\omega}{\varphi} + \frac{\varphi \alpha_{\text{opt}}^*}{2} \right) \\ &= -\frac{2(1 - \xi) \alpha_{\text{opt}}^*}{\theta T \xi} \left(\frac{1}{T} \left(\sqrt{1 + \frac{\gamma \bar{P} T}{NN_0}} - 1 \right) + \frac{\varphi \alpha_{\text{opt}}^*}{2} \right) \end{aligned} \quad (66)$$

Combining (66) and (63), we can prove (40). \square

REFERENCES

- [1] S. Verdú, "Spectral efficiency in the wideband regime," *IEEE Trans. Inform. Theory*, vol.48, no.6 pp.1319-1343. Jun. 2002.
- [2] A. Ephremides and B. Hajek, "Information theory and communication networks: An unconsummated union," *IEEE Trans. Inform. Theory*, vol. 44, pp. 2416-2434, Oct. 1998.
- [3] S. V. Hanly and D.N.C Tse, "Multiaccess fading channels-part II: delay-limited capacities," *IEEE Trans. Inform. Theory*, vol.44, no.7, pp.2816-2831. Nov. 1998.
- [4] D. Wu and R. Negi "Effective capacity: a wireless link model for support of quality of service," *IEEE Trans. Wireless Commun.*, vol.2,no. 4, pp.630-643. July 2003

- [5] D. Wu and R. Negi, "Downlink scheduling in a cellular network for quality-of-service assurance, *IEEE Trans. Veh. Technol.*, vol.53, no.5, pp. 1547-1557, Sep., 2004.
- [6] D. Wu and R. Negi, "Utilizing multiuser diversity for efficient support of quality of service over a fading channel, *IEEE Trans. Veh. Technol.*, vol.49, pp. 1073-1096, May 2003.
- [7] J. Tang and X. Zhang, "Quality-of-service driven power and rate adaptation over wireless links, *IEEE Trans. Wireless Commun.*, vol. 6, no. 8, pp.3058-3068, Aug. 2007.
- [8] J. Tang and X. Zhang, "Quality-of-service driven power and rate adaptation for multichannel communications over wireless links, *IEEE Trans. Wireless Commun.*, vol. 6, no. 12, pp.4349-4360, Dec. 2007.
- [9] J. Tang and X. Zhang, "Cross-layer modeling for quality of service guarantees over wireless links, *IEEE Trans. Wireless Commun.*, vol. 6, no. 12, pp.4504-4512, Dec. 2007.
- [10] J. Tang and X. Zhang, "Cross-layer-model based adaptive resource allocation for statistical QoS guarantees in mobile wireless networks, *IEEE Trans. Wireless Commun.*, vol. 7, pp.2318-2328, June 2008.
- [11] L. Liu, P. Parag, J. Tang, W.-Y. Chen and J.-F. Chamberland, "Resource allocation and quality of service evaluation for wireless communication systems using fluid models," *IEEE Trans. Inform. Theory*, vol. 53, no. 5, pp. 1767-1777, May 2007
- [12] L. Liu, P. Parag, and J.-F. Chamberland, "Quality of service analysis for wireless user-cooperation networks," *IEEE Trans. Inform. Theory*, vol. 53, no. 10, pp. 3833-3842, Oct. 2007
- [13] L. Liu, and J.-F. Chamberland, "On the effective capacities of multiple-antenna Gaussian channels," *IEEE International Symposium on Information Theory*, Toronto, 2008.
- [14] M.C. Gursoy, D. Qiao, and S. Velipasalar, "Analysis of energy efficiency in fading channel under QoS constrains," accepted to the *IEEE Trans. Wireless Commun.*, 2009; conference version to appear at the *IEEE Global Communications Conference (GLOBECOM)*, Dec. 2008.
- [15] D. Qiao, M.C. Gursoy, and S. Velipasalar, "The impact of QoS constraints on the energy efficiency of fixed-rate wireless transmissions," submitted to the *IEEE Trans. Wireless Commun.*, 2008; conference version to appear at the *IEEE International Conference on Communications (ICC)*, Jun. 2009.
- [16] C.-S. Chang, "Stability, queue length, and delay of deterministic and stochastic queuing networks," *IEEE Trans. Auto. Control*, vol. 39, no. 5, pp. 913-931, May 1994
- [17] C.-S. Chang, *Performance Guarantees in Communication Networks*, New York: Springer, 1995
- [18] P. Sadeghi and P. Rapajic, "Capacity analysis for finite-state Markov mapping of flat-fading channels," *IEEE Trans. Commun.* vol. 53, pp. 833-840, May 2005.
- [19] L. Tong, B. M. Sadler, and M. Dong, "Pilot-assisted wireless transmission," *IEEE Signal Processing Mag.*, pp. 12-25, Nov. 2004.
- [20] B. Hassibi and B. M. Hochwald, "How much training is needed in multiple-antenna wireless links", *IEEE Trans. Inform. Theory*, vol. 49, pp. 951-963, Apr. 2003.
- [21] M. C. Gursoy, "On the capacity and energy efficiency of training-based transmissions over fading channels," submitted for publication. Available online at <http://arxiv.org/abs/0712.3277>.
- [22] A. Lapidoth and S. Shamai (Shitz), "Fading channels: How perfect need 'perfect side information' be?," *IEEE Trans. Inform. Theory*, vol. 48, pp. 1118-1134, May 2002.
- [23] D. Porrat, D. N. C. Tse, and S. Nacu, "Channel uncertainty in ultra-wideband communication systems," *IEEE Trans. Inform. Theory*, vol. 53, pp. 194-208, Jan. 2007.
- [24] V. Raghavan, G. Hariharan, and A. M. Sayeed, "Capacity of sparse multipath channels in the ultra-wideband regime," *IEEE Journ. Select. Topics in Signal Processing*, vol. 1, pp. 357-371, Oct. 2007.
- [25] E. Telatar and D. N. C. Tse, "Capacity and mutual information of wideband multipath fading channels," *IEEE Trans. Inform. Theory*, vol. 46, pp. 1384-1400, July 2000.
- [26] A. Goldsmith, *Wireless Communications*, 1st ed. Cambridge University Press, 2005.
- [27] Tim Szigeti and Christina Hattingh, *End-to-End QoS Network Design: Quality of Service in LANs, WANs, and VPNs*, Cisco Press, 2004.
- [28] M. H. Protter, C. B. Morrey, and C. B. Morrey, Jr., *A First Course in Real Analysis*, 2nd ed., Springer, 1991.
- [29] G. R. Grimmett and D. R. Stirzaker, *Probability and Random Processes*, 2nd ed. Oxford University Press, 1998.
- [30] I. S. Gradshteyn and I. M. Ryzhik, *Table of Integrals, Series, and Products*, Academic Press, 2000.

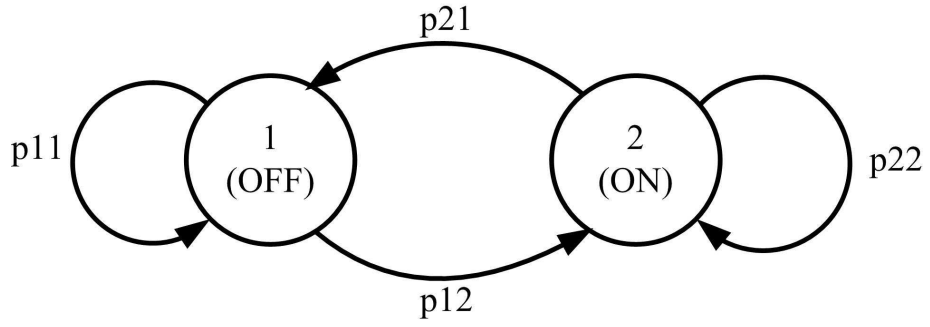


Fig. 1. ON-OFF state transition model.

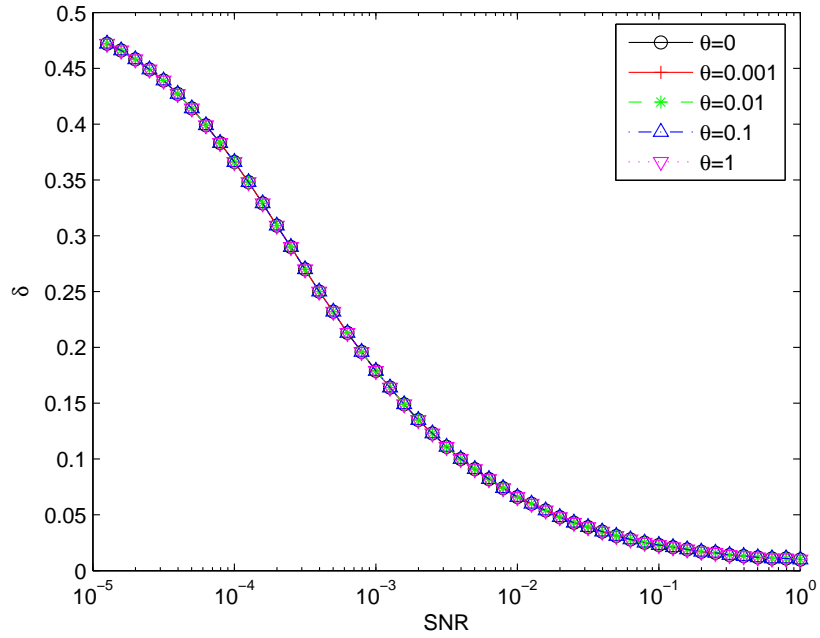


Fig. 2. Optimal portion ρ_{opt} vs. SNR in the Rayleigh channel. $B = 10^7$ Hz.

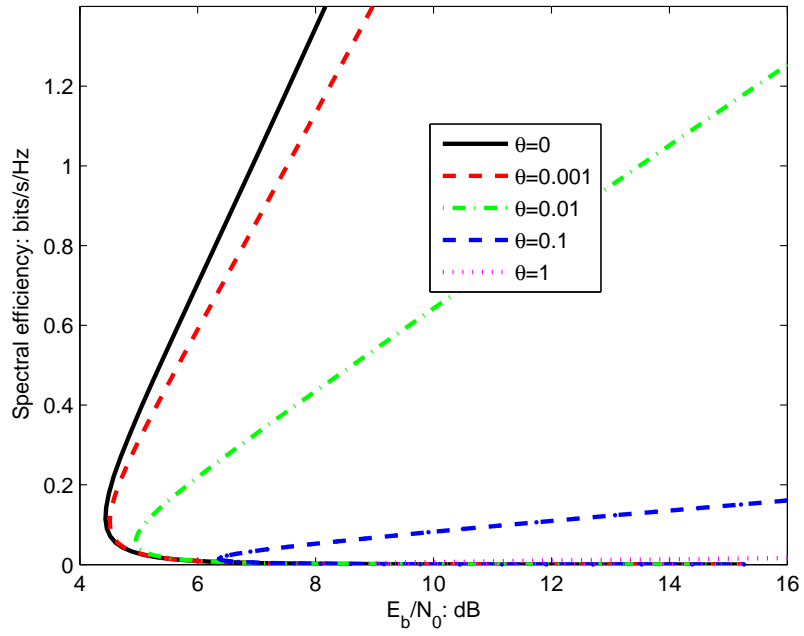


Fig. 3. Spectral efficiency vs. E_b/N_0 in the Rayleigh channel. $B = 10^5$.

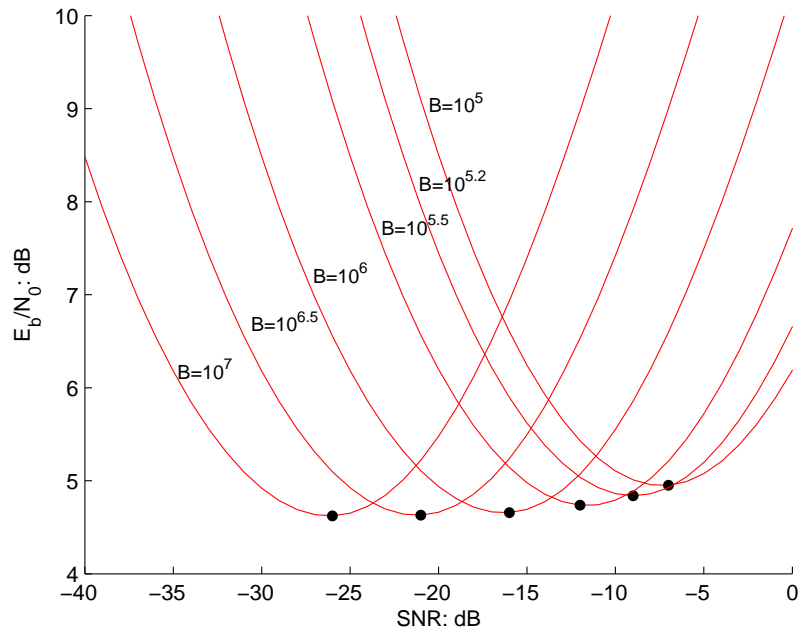


Fig. 4. E_b/N_0 vs. SNR in the Rayleigh channel. $\theta=0.01$.

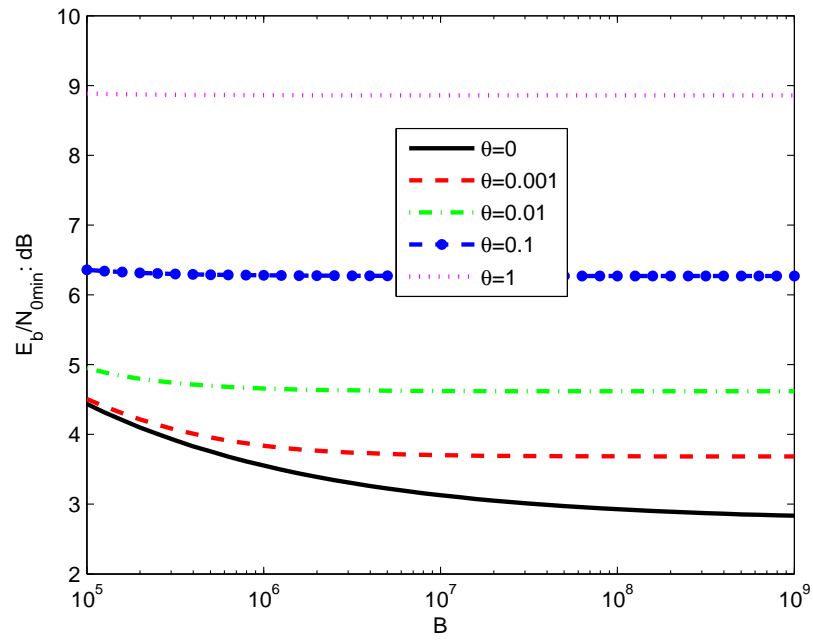


Fig. 5. $\frac{E_b}{N_0}_{\min}$ vs. B in the Rayleigh channel.

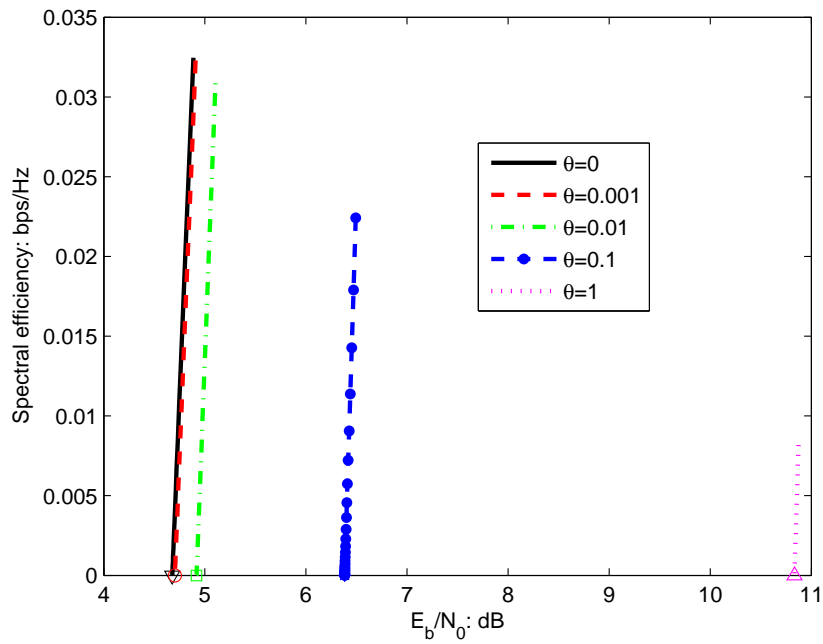


Fig. 6. Spectral efficiency vs. E_b/N_0 in the Rayleigh channel with $E\{|h|^2\} = \gamma = 1$. $\bar{P}/NN_0 = 10^4$.

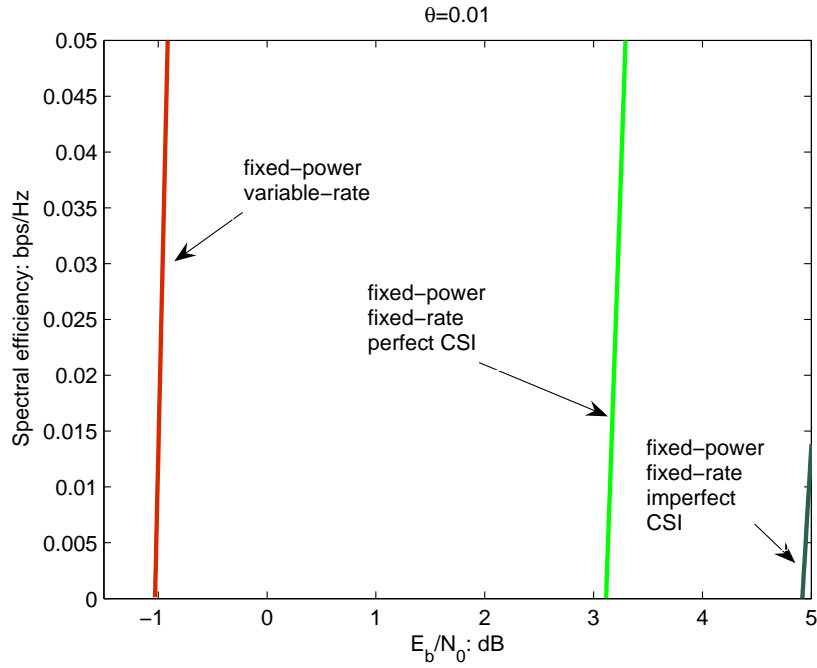


Fig. 7. Comparison of spectral efficiency; $\bar{P}/NN_0 = 10^4$, $\theta = 0.01$, and $E\{|h|^2\} = \gamma = 1$.

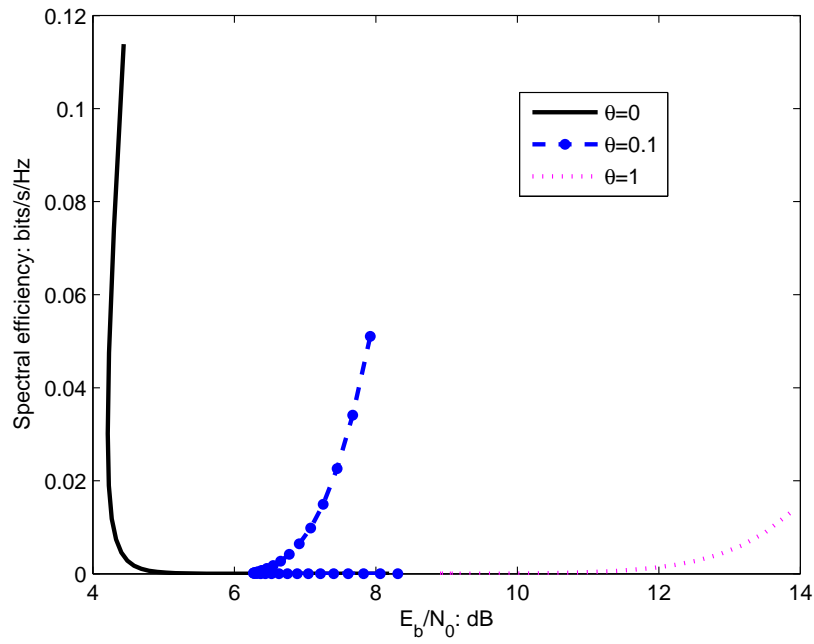


Fig. 8. Spectral efficiency vs. E_b/N_0 in the Rayleigh channel with $E\{|h|^2\} = \gamma = 1$. $\bar{P}/NN_0 = 10^4$.